

## Recent Advances in Modelling Creep Crack Growth

H. RIEDEL

*Fraunhofer-Institut für Werkstoffmechanik, Wöhlerstr. 11,  
Freiburg, FRG*

### ABSTRACT

At the time of the previous International Conference on Fracture, the  $C^*$  integral had long been recognized as a promising load parameter for correlating crack growth rates in creep-ductile materials. The measured crack growth rates as a function of  $C^*$  and of the temperature could be understood on the basis of micromechanical models. The distinction between  $C^*$ -controlled and  $K_I$ -controlled creep crack growth had been clarified and first attempts had been made to describe creep crack growth in the transient regime between elastic behavior and steady-state creep.

This paper describes the progress in describing transient crack growth including the effect of primary creep. The effect of crack-tip geometry changes by blunting and by crack growth on the crack-tip fields and on the validity of  $C^*$  is analyzed by idealizing the growing-crack geometry by a sharp notch and using recent solutions for the notch-tip fields. A few new three-dimensional calculations of  $C^*$  are cited and important theoretical points are emphasized regarding the three-dimensional fields at crack tips. Finally, creep crack growth is described by continuum-damage models for which similarity solutions can be obtained. Crack growth under small-scale creep conditions turns out to be difficult to understand. Slightly different models yield very different crack growth rates.

### KEYWORDS

Creep crack growth, high-temperature fracture, fracture mechanics,  $C^*$  integral, damage mechanics.

## INTRODUCTION

Creep crack growth is the slow extension of a macroscopic crack, which usually, but not necessarily, occurs along grain boundaries by the formation of creep cavities ahead of the crack tip. Local corrosion in the crack-tip zone often plays an additional role.

Creep crack growth may or may not be rate controlling for the lifetime of a component operating at high temperatures. At present it appears that in the majority of technologically important cases, creep crack growth plays no predominant role. For example, if seamless pipe bends in fossil-fired electric power-generating plants fail, they do so by a more or less homogeneous cavitation of grain boundaries over large portions of the pipe. According to the long-term experience with these pipes in Europe, small defects do not reduce the lifetime considerably, since crack growth from small defects takes longer than does failure by cavitation. Incidentally, it should be noted that grain boundary cavitation eventually leads to cracks, but this is not a typical example of what we understand to be creep crack growth. First the growth of these cracks occupies only a small fraction of the lifetime, so that it is often practically irrelevant, and second these cracks grow through material that is already heavily damaged, whereas the usual methods of dealing with creep crack growth rely on a small-scale damage assumption.

However, the experience with pipes in power plants should not lead to the conclusion that creep crack growth may generally be ignored as a potential failure mode in all cases. For example, the failure of pipes with a longitudinal seam weld has been treated as a problem of creep crack growth (Viswanathan, Dooley and Saxena, 1988). In general, the danger of premature failure by crack growth is greater in creep brittle materials, for large and inhomogeneously stressed components (like at notches), for large pre-existing defects, or if cracks are nucleated by some other mechanism such as fatigue, corrosion or thermal shock.

Since the late 1960's, creep crack growth rates have been measured, primarily in ferritic steels for applications in steam turbine components and other power plant equipment (e.g. Sivers and Price, 1970; Harrison and Sandor, 1971; Nikbin, Webster and Turner, 1976; Taira, Ohtani and Kitamura, 1979; Ohji, Ogura, Kubo and Katada, 1980; Gooch, 1982; Riedel and Wagner, 1984; Koterazawa, 1986; Riedel and Detampel, 1987), in austenitic steels for piping and pressure vessel applications (Koterazawa and Mori, 1977; Ohji *et al.*, 1978, 1980; Taira *et al.*, 1979; Saxena, 1980; Sadananda and Shahinian, 1980a, 1980b, 1983; Maas and Pineau, 1985; Jaske, 1988; Hollstein and Kienzler, 1988), and in nickel-base alloys primarily for gas turbines (Landes and Begley, 1976; Sadananda and Shahinian, 1980a, 1983; Floreen, 1983; Kienzler and Hollstein, 1987). Fewer papers have appeared on cobalt alloys (Sadananda and Shahinian, 1983) on aluminum alloys (Nikbin, Webster and Turner, 1976; Radhakrishnan and McEvily, 1980; Webster, Smith and Nikbin, 1986), and on ceramic materials (Evans and Blumenthal, 1982). A comparison of many different materials was given by Speidel (1981). More references

can be found in the recent literature and in previous reviews (Riedel, 1985a, 1987). The results are stored in data banks.

In the following sections, theoretical results will be presented without giving any derivations. The underlying equations are the continuum-mechanical equations for the equilibrium of the stress field, for the compatibility of the strain field and various material laws specified in the respective sections. The tools to derive the results are almost exclusively very simple ones: the scaling properties of power-law materials are exploited; dimensional considerations are used to analyse limiting cases, between which one can interpolate; the exact or approximate path independence of the J integral or related quantities is utilized; few finite-element results are employed to check analytical approximations numerically. For more details, the reader is referred to the original literature which is quoted.

## STATE OF THE ART UP TO THE TIME OF ICF6

### Nonlinear Viscous Material and the C\* Integral

In the middle 1970's it was recognized that the viscous analogue of the J integral (Rice, 1968), which was subsequently called C\*, J', J\* or J, should be an appropriate load parameter to correlate creep crack growth rates in different types of specimens and components (Ohji *et al.*, 1974; Landes and Begley, 1976; Nikbin *et al.*, 1976). The prerequisite for this to be true is that the material is purely viscous, i.e. the strain rate must be an unequivocal, but arbitrary, function of stress. A specific form is Norton's power law

$$\dot{\epsilon} = A \sigma^n \quad (1)$$

which is convenient for analytical purposes. But this specific stress-strain rate relation is not a prerequisite for the validity of C\*.

Since viscous deformation corresponds to secondary, or steady-state creep, which often determines the creep behavior of real materials to within a good approximation, it is not surprising that C\* was found to be rather successful in correlating crack growth rates measured in specimens of different sizes and shapes.

An important tool for the application of C\* has been the Plastic Fracture Handbook (Kumar, German and Shih, 1981) which provides tables for the calculation of the J integral for power-law hardening materials based on finite element solutions for various specimen geometries. Due to the elastic-viscous analogy these results can directly be used for C\* in power-law viscous materials as well. The general form of C\* must be

$$C^* \propto a A \sigma^{n+1} \quad (2)$$

where a is crack length,  $\sigma$  is a measure of the applied stress in the cracked specimen (e.g. net section stress or reference

stress), and the factor of proportionality which is not given in eq. (2), depends on the choice of that stress measure, and is tabulated by Kumar et al. (1981). A convenient way of determining  $C^*$  is to introduce the deflection rate at the loading points,  $\dot{\Delta} \propto A \sigma^n$  with the factor of proportionality being given by Kumar et al. Together with eq. (2) this gives

$$C^* = g_2 \sigma_{net} \dot{\Delta} \quad (3)$$

The dimensionless factor  $g_2$  depends on the specimen geometry and on  $n$ . The advantage of eq. (3) over (2) is that it is relatively insensitive to the value of  $n$  and to plane strain or plane stress. Both,  $n$  and the state of stress are often not exactly known in creep crack growth experiments.

Since  $C^*$  is a path-independent integral in viscous materials, it can not only be measured at the loading points of the specimen, but it also determines the stress and strain rate fields at the crack tip. For the special case of power-law viscous materials the crack-tip field is an HRR field (Hutchinson, 1968; Rice and Rosengren, 1968):

$$\sigma_{ij} = \left[ \frac{C^*}{I_n A r} \right]^{1/(n+1)} \tilde{\sigma}_{ij}(\theta) \quad (4)$$

The dimensionless quantities  $I_n$  and  $\tilde{\sigma}_{ij}(\theta)$  have been tabulated by Shih (1983), and  $r$  and  $\theta$  are polar coordinates centered at the crack tip.

Despite the success of  $C^*$  in several investigations, limitations to  $C^*$  must be expected to become effective once the material deviates significantly from a nonlinear viscous behavior, or if significant crack-tip blunting occurs. The term "significant" will be specified under various aspects later.

#### Crack Growth Rates in Power-Law Viscous Material

In the early 1980's models for creep crack growth were developed based on grain boundary cavitation ahead of the crack tip (Riedel, 1981a; Bassani, 1981). Good agreement with measured crack growth rates was obtained if cavity nucleation and growth were assumed to be strain controlled. Then, instead of considering cavities ahead of the crack, one can equivalently require that the crack grows subject to a critical-strain criterion. A similar model had been described earlier by Kubo et al. (1979). Such a model predicts that the crack starts growing after an incubation time

$$t_i = \left[ \frac{I_n A x_c}{C^*} \right]^{n/(n+1)} \frac{\epsilon_c}{A (\tilde{\sigma}_e(0))^n} \quad (5)$$

where  $\epsilon_c$  is the critical strain pertinent to the triaxial stress field at the crack tip and  $x_c$  is a structural length ahead of the crack tip at which the critical strain is to be attained;  $\sigma(0)$  is the value of the angular function appearing in eq. (4) for the equivalent tensile stress at  $\theta=0$ .

After crack growth initiation the evolution of the growth rate is described by an integral equation resulting from the integration of the strain rate over the prior history at a generic point ahead of the crack. The crack growth rate must have the general form

$$\dot{a} = \frac{(\tilde{\sigma}_e(0))^n}{I_n^{n/(n+1)}} \frac{(A x_c)^{1/(n+1)}}{\epsilon_c} C^{*n/(n+1)} f(\Delta a/x_c) \quad (6)$$

where  $\Delta a$  is the amount of crack growth since the beginning of the test, and the dimensionless function  $f(\Delta a/x_c)$  results from the solution of the integral equation. In general this solution can be obtained numerically. Useful two-term expansions for small and large  $\Delta a/x_c$  are, respectively,

$$f(\Delta a/x_c) = \frac{n+1}{n} \left( 1 + \frac{\Delta a}{x_c} \right) \quad (7a)$$

$$f(\Delta a/x_c) = \frac{\pi}{\sin(\pi n/(n+1))} \left[ \left( \frac{\Delta a}{x_c} \right)^{1/(n+1)} - \gamma_n \right] \quad (7b)$$

The dimensionless quantity  $\gamma_n$  can be expressed in terms of Gamma functions (see, for example, Riedel, 1987) and has numerical values between 0.85 and 1 for  $n = 4$  to  $\infty$ .

In numerous experiments, the predicted proportionality of  $\dot{a}$  on the  $n/(n+1)$ 'th power of  $C^*$  has been confirmed. The temperature enters into eq. (6) primarily through the creep coefficient  $A$ , which is, however, raised to the small power  $1/(n+1)$ , so that the predicted temperature dependence of the  $\dot{a}$ - $C^*$  relation is weak. This is indeed confirmed by experiments (e.g., Riedel and Wagner, 1984). (Of course, the growth rate is strongly temperature-dependent if tests at a fixed load, rather than at a fixed  $C^*$ , are compared.) Finally, eqs. (6) and (7) predict that, beyond the dependence on  $C^*$ , the growth rate should increase as a function of  $\Delta a$ , the rate of increase becoming very small at large  $\Delta a$  according to eq. (7b). Such an additional dependence of  $\dot{a}$  has been observed qualitatively in almost all creep crack growth tests. Semi-quantitative comparisons with experiments by Maas and Pineau (1984) and by Riedel and Wagner (1984) gave a fair agreement. It should be noted, however, that transients to be described later are superimposed on the crack growth behavior described so far, so that the initial increase of  $\dot{a}$  as a function of  $\Delta a$  may be masked.

In the derivation of eqs. (5) to (7) it was assumed that the cavities do not disturb the HRR field, which prevails at crack tips in power-law viscous materials. In the damage-mechanics

approach to be described later, this assumption is dropped. Nevertheless, the results for the crack growth rate are virtually the same.

Elastic/Nonlinear Viscous Material.  $K_I$  vs.  $C^*$

As a prototype problem of bounding the range of validity of  $C^*$  against that of an other load parameter, Riedel and Rice (1980) and Ohji, Ogura and Kubo (1980) considered an elastic/power-law viscous material described in uniaxial tension by  $\dot{\epsilon} = \dot{\sigma}/E + A\sigma^n$ , where  $E$  is Young's modulus. For short times, large creep strains in such a material are confined to a small creep zone, which grows around the crack tip according to

$$r_{cr} \propto K_I^2 (EAt)^{2/(n-1)} \quad (8)$$

In this short-time, or small-scale-creep limit, the specimen behaves predominantly elastic and  $K_I$  is the load parameter to describe the evolution of the fields near the crack tip. After long times, creep strain dominates compared to elastic strain on the whole ligament of the specimen. The specimen behaves as if it were purely nonlinear viscous and hence  $C^*$  is applicable. The characteristic time that separates the regimes of  $K_I$  and  $C^*$  is

$$t_1 = \frac{K_I^2 (1-\nu^2)/E}{(n+1) C^*} \quad (9)$$

At the time of the Sixth International Conference on Fracture the practical value of  $t_1$  for choosing the appropriate load parameter under given testing conditions had been demonstrated repeatedly (e.g. Ohji, Ogura, Kubo and Katada, 1980; Riedel and Wagner, 1984).

It had also been recognized that the transient from the initial elastic to the steady-state creep response plays a role in many experiments. To describe crack growth rates in the transient regime, Saxena and Landes (1984) and Saxena (1986) introduced the  $C_t$  parameter. This parameter is measured using essentially the same formula as that for  $C^*$ , eq. (3). However, eq. (3) is meaningless for  $C^*$  outside the steady-state creep regime, whereas it gives  $C_t$  during the transient as well. (There has been some confusion in the literature, since several workers denote the result of eq. (3) by  $C^*$  irrespective of whether or not steady-state creep prevails. Others, including the present author, suggest the use of  $C^*$  only under steady-state creep conditions, i.e. in effectively nonlinear viscous materials).

In the following sections, the further developments after ICF6 in the area of transient creep crack growth, as well as in other areas, are reviewed.

The Amplitude of the HRR Field,  $C(t)$

If the crack tip is surrounded by a creep zone in which power-law, secondary creep dominates, the asymptotic field near the crack tip is an HRR field of the form

$$\sigma_{ij} = \left[ \frac{C(t)}{I_n A r} \right]^{1/(n+1)} \tilde{\sigma}_{ij}(\theta) \quad (10)$$

For steady-state creep of the whole specimen,  $C(t)$  approaches its steady-state value,  $C^*$ . It remains to calculate  $C(t)$  during the transient as a function of the time and of the load, which will be done shortly.

As Riedel (1987) has shown, the micromechanical models of creep crack growth based on grain boundary cavitation can readily be generalized to time-dependent  $C(t)$ , as opposed to a constant  $C^*$ . The crack growth rate is then given by eqs.(6) and (7) with  $C^*$  replaced by  $C(t)$ , i.e.  $\dot{a} \propto C(t)^{n/(n+1)}$ . Hence, at least in the framework of these models, crack growth rates should correlate with  $C(t)$  during the transient in the same way as they correlate with  $C^*$  in the steady state.

Since  $C(t)$  is not a path-independent integral, except in the limiting case when it is equal to  $C^*$ , it cannot be directly measured at the loading points of the specimen. Therefore, a theoretical analysis is needed to determine  $C(t)$ .

Calculation of  $C(t)$  for Elastic/Nonlinear Viscous Materials

For elastic/nonlinear viscous materials Ehlers and Riedel (1981) have shown by finite element calculations that the formula

$$C(t) = (t_1 / t + 1) C^* \quad (11)$$

approximates the numerical results closely at all times. For short times, eq. (11) reproduces the analytical results of Riedel and Rice (1980), whereas for long times it correctly approaches  $C^*$ . This result was confirmed repeatedly, most recently by a detailed finite-element study of Li, Needleman and Shih (1988).

If the initial material response is elastic-plastic, rather than only elastic, it was suggested that  $C(t)$  retains the form of eq. (11), but in eq. (9),  $K_I^2(1-\nu^2)/E$  should be replaced by the  $J$  integral to calculate  $t_1$ .

### Comparison of $C(t)$ and $C_t$ for Elastic/Nonlinear Viscous Material

Various authors noticed that the short-time behavior of  $C_t$  is not equal but similar to that of  $C(t)$  (Riedel, 1987; Kuhnle and Riedel, 1987; Leung et al, 1988a,b). By an argument analogous to the plastic-zone correction argument in elastic-plastic fracture mechanics one concludes that in small-scale creep the load-line deflection rate, and hence  $C_t \propto \dot{\Delta}$ , must be proportional to the growth rate of the creep zone  $\dot{\epsilon}$ , which, according to eq. (8), is  $\dot{\epsilon}_{cr} \propto t^{-(n-3)/(n-1)}$ . The interpolation formula

$$C_t = \left[ \alpha (t_1/t)^{(n-3)/(n-1)} + 1 \right] C^* \quad (12)$$

approximates the finite element results of Ehlers (1981) well for all times with  $\alpha = 0.77$  for three-point bend and double-edge-cracked tension specimens and  $\alpha = 1.23$  for CT-specimens, all with  $a/W = 0.5$  and  $n=5$ . Comparison of eqs. (11) and (12) shows that  $C_t$  indeed approximates  $C(t)$  if  $n$  is large and if  $\alpha$  is of the order unity. Although this condition for  $\alpha$  is fulfilled for the test specimen configurations mentioned above, it cannot be generalized without care. In a specimen with a small crack, for example,  $\alpha$  must become very small if the displacement rate is measured far from the crack, but it may have a value near unity if the displacement rate is measured near the crack.

### Primary-Creep Effects on $C(t)$

Recent experiments, to be described later, indicate that the elastic transients discussed so far are insufficient to explain the observed transient behavior. Hence primary creep is taken into account to improve the theoretical description.

A constitutive equation, which exhibits the necessary features to describe the experiments but is simple enough to allow for approximate closed-form solutions is (for uniaxial tension)

$$\dot{\epsilon} = \dot{\sigma}/E + A_0 \sigma^{1/N-1} \dot{\sigma} + A_1 \sigma^{m(1+p)} \epsilon^{-p} + A_2 \sigma^n \quad (13)$$

where the four terms represent elastic, instantaneous plastic, primary-creep and secondary-creep deformation, respectively. In particular,  $N$  is the hardening exponent for instantaneous plasticity, and  $p$  is the strain hardening exponent in primary creep. A typical value is  $p=2$ , in which case eq. (13) gives Andrade's primary creep law,  $\epsilon \propto t^{1/3}$ , upon integration for constant stress.

Depending on the values of the material parameters and of the load, the fields in a cracked specimen can develop in different ways. The primary-creep zone, which grows in the initial elastic-plastic fields may either be overtaken by the secondary-creep zone while both are still small, so that primary creep never plays a great role for the overall behavior of the specimen; or the primary-creep zone may spread though the whole specimen while the secondary-creep zone is still small. The

characteristic time for the transition from the initial elastic-plastic state to extensive primary creep of the whole specimen is

$$t_1 = \frac{1}{m+1} \left[ \frac{J}{C_h^*} \right]^{1+p} \quad (14)$$

The time for the transition from primary to secondary creep is

$$t_2 = \left[ \frac{C_h^*}{(p+1)C^*} \right]^{(p+1)/p} \quad (15)$$

Here  $C_h^*$  is the analogue of  $C^*$  for a specimen deforming in primary creep only (Riedel, 1981b).

The HRR-field amplitude during the transient can be described by the approximate interpolation formula

$$C(t) = \left[ t_1/t + (t_2/t)^{p/(p+1)} + 1 \right] C^* \quad (16)$$

with  $t_1$  from eq. (9), rather than from eq. (14). Equation (16) has the correct behavior in the small-scale creep limit, i.e. when  $t \ll t_1 (t_1/t_2)^p$ , for predominantly primary creep of the whole specimen, i.e., when  $t_1 \ll t \ll t_2$ , and for extensive secondary creep, i.e. when  $t \gg t_2$ .

### Comparison of $C(t)$ and $C_t$ for Primary Creep

If primary creep dominates in the whole specimen except possibly in a small secondary-creep zone, the load line deflection rate is given by

$$\dot{\Delta} = a \frac{A_1^{1/(p+1)} \sigma_{ref}^m}{((p+1)t)^{p/(p+1)}} h_3(a/W, m) \quad (17)$$

The dimensionless function  $h_3$  and the reference stress  $\sigma_{ref}$  are given by Kumar et al. (1981).<sup>3</sup> For the CT specimen, for example,  $\sigma_{ref} = \sigma_{net} / (1.455\eta)$ , where  $\sigma_{net}$  is load divided by uncracked ligament area,  $\eta$  is a given function of  $a/W$ , and the numerical factor is valid for plane strain; for plane stress the factor is 1.071.

Calculating  $C_t$  from eq. (3) with eq. (17) inserted shows that  $C_t$  is exactly equal to  $C(t)$  under primary-creep conditions, i.e. when the middle term in brackets in eq. (16) dominates. This result has been mentioned by Kuhnle and Riedel (1987) and has been confirmed numerically by Leung, McDowell and Saxena (1988b).

Hence,  $C_t$  and  $C(t)$  are nearly equal in the whole time range except for the reservations made in the paragraph following eq. (12). This means that  $C_t$  is a reasonable measure for the crack-tip fields and, at  $t$  the same time, it can be measured conveniently.

#### Comparison with Experiments Involving Primary Creep

Primary-creep effects can be observed in the load-line deflection rate and in the crack growth rate. Riedel and Detampel (1987) find for two ferritic steels that the displacement during the transient increases as  $\Delta - \Delta_0 \propto t^{1/3}$  which is exactly compatible with the primary-creep behavior of the materials. During the elastic transient one would expect  $\Delta - \Delta_0 \propto t^{2/(n-1)}$  ( $= t^{0.15}$  for the stress exponent of one of the steels,  $n=14$ ). Similarly, Leung, McDowell and Saxena (1988b) can explain the deflection rates measured on another ferritic steel only if they take primary creep into account in their finite element analysis.

Riedel (1987) and Riedel and Detampel (1987) compare experimental crack growth histories with calculated ones. An example for 1/2Cr-1/2Mo-1/4V steel is reproduced next.

As mentioned earlier, the crack growth rate is related to  $C(t)$ , eq. (16), as  $\dot{a} \propto C(t)^{n/(n+1)}$ . The crack length as a function of time is obtained by numerical integration of the crack growth law (numerical since  $C^*$  is given numerically as a function of the crack length). The result, which is shown in Fig.1, was obtained with the following material parameters.

$$\begin{array}{lll} A_1 = 5 \cdot 10^{-61} (\text{MPa})^{-3m}/s & m = 7.3 & p = 2 \\ A = 1.7 \cdot 10^{-39} (\text{MPa})^{-n}/s & n = 14.1 & \\ A_0 = 9 \cdot 10^{-15} (\text{MPa})^{-1/N} & N = 0.2 & \\ E = 172 \text{ GPa} & \nu = 0.3 & \epsilon_c = 1.2\% \end{array}$$

The value of the critical strain,  $\epsilon_c$ , was chosen such that the calculated lifetime coincides with the observed one (1,456 hours in this case).

From these material parameters, from the load  $P = 4.51\text{kN}$  and the CT-specimen geometry, the load parameters can be determined using the Plastic Fracture Handbook of Kumar et al. (1981):

$$J = 5 \text{ kJ/m}^2 \quad C^* = 3.9 \cdot 10^{-3} \text{ W/m}^2 \quad C_h^* = 100 \text{ J/(m}^2 \text{ s}^{1/3}).$$

These values were calculated assuming plane strain and considering the net specimen thickness between the side grooves as the relevant thickness, since a comparison with the three-dimensional finite element analysis of deLorenzi and Shih

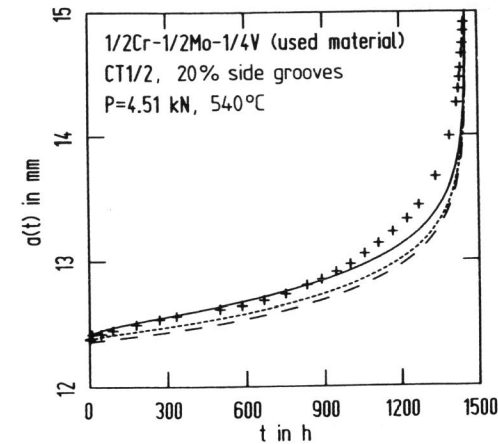


Fig. 1. The evolution of the crack length (after Riedel and Detampel, 1987).  
Solid line: Calculated with  $t_1 = 24\text{h}$ ,  $t_2 = 230\text{h}$ .  
Dotted line:  $t_1 = 24\text{h}$ ,  $t_2 = 0$ . Dashed line:  $t_1 = t_2 = 0$ .

(1983), showed that this choice gives the best two-dimensional estimate for side-grooved specimens.

From the load parameters one calculates the characteristic times to be  $t_1 = 24\text{h}$  (from eq. (9) for the transition from elastic-plastic to secondary creep),  $t_1 = 4\text{h}$  (from eq. (14) for the transition from elastic-plastic to primary creep),  $t_2 = 230\text{h}$  (from eq. (15) for the transition from primary to secondary creep).

As Fig. 1 shows, the initial behavior of the crack growth rate is described accurately by the theoretical prediction if primary creep is taken into account (the solid line in Fig. 1). To illustrate the importance of primary creep, the dotted line was calculated neglecting primary creep by setting  $t_2 = 0$  in eq. (16). (The lifetime was fitted by choosing  $\epsilon_c = 0.7\%$ ). Finally, the elastic-plastic transient was neglected also by setting  $t_1 = 0$  and  $t_2 = 0$ , which leads to the dashed curve (with  $\epsilon_c = 0.6\%$ ). Obviously, primary creep is necessary to explain the initial transient behavior.

#### CRACK-TIP GEOMETRY CHANGES BY BLUNTING AND BY CRACK GROWTH

In this section the profile of a crack is calculated which blunts and grows in a power-law viscous material. The calculation starts from the stress field of a sharp crack, i.e.

the HRR field, eq. (4). Crack-tip geometry changes are thus initially neglected, but the consequences of this approximation are discussed at the end. It should further be noted that in a viscous material the stress field is independent of whether the crack is stationary or whether it grows. Only the current crack length enters into the calculation of the stress field.

The incentive to analyse the blunting of a crack tip is to explore the range of validity of  $C^*$  as a correlating parameter. In analogy to  $J$  in rate-independent fracture mechanics (Hutchinson and Paris, 1979),  $C^*$  can only be a valid parameter if the crack-tip field (the HRR field in power-law materials) has a finite range of approximate validity between its outer limitation, which is a certain geometry-dependent fraction of the crack length, and the disturbance by blunting.

### Calculation of the Crack Profile

Within the approximation that geometry changes are neglected the crack profile is calculated by integrating the HRR displacement rate field

$$\dot{u}_i = (Ar)^{1/(n+1)} (C^*/I_n)^{n/(n+1)} \tilde{u}_i(\theta) \quad (18)$$

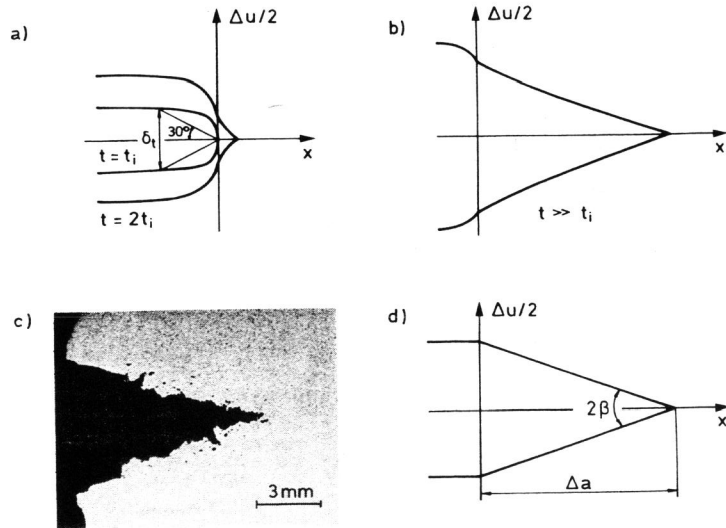


Fig. 2. Crack profiles:  
a and b) Calculated for  $n = 7$ ,  $\epsilon_c = 3\%$ .  
c) Experimental in  $2\frac{1}{4}\text{Cr-1Mo}$  steel at  $540^\circ\text{C}$ .  
d) Idealized sharp notch geometry.

The dimensionless angular function  $\tilde{u}_i(\theta)$  was tabulated by Shih (1983). For a stationary crack, the blunted crack profile is calculated as  $\Delta u = 2\dot{u}_\theta(\pi)t$ . This is shown by the line denoted by  $t=t_i$  in Fig. 2. The crack-tip opening displacement,  $\delta_t$ , can be defined where the two lines through the apex of the crack tip inclined by  $\pm 30^\circ$  intersect the crack profile. This definition is illustrated in Fig.2 and gives

$$\delta_t = \left[ \frac{2|\tilde{u}_\theta(\pi)|^{1+1/n}}{(\tan 30^\circ)^{1/n} I_n} \right] A^{1/n} C^* t^{1+1/n} \quad (19)$$

The term in square brackets is equal to 1.25 and 1.11 for  $n = 5$  and 7, respectively.

After crack growth initiation, the crack profile is given by an integral of the displacement rate over the prior crack growth history with the time differential,  $dt$ , being replaced by  $d(\Delta a)/\dot{a}(\Delta a)$ :

$$\Delta u = 2A\tilde{u}_\theta(\pi) \left[ \frac{C^*}{I_n A} \right]^{n/(n+1)} \begin{cases} \int_x^{\Delta a} \frac{(a'-x)^{1/(n+1)}}{\dot{a}(a')} da' & (\text{for } x>0) \\ \int_0^{\Delta a} \frac{(a'-x)^{1/(n+1)}}{\dot{a}(a')} da' + (-x)^{1/(n+1)} t_i & (\text{for } x<0) \end{cases} \quad (20)$$

The coordinate  $x$  is measured from the original crack tip in the direction of crack growth, and  $t_i$  is the crack growth initiation time. If crack growth is controlled by a critical-strain criterion,  $t_i$  is given by eq. (5). For very small crack growth increments,  $\Delta a$ , the crack growth rate can be approximated by the initial value of the rate given in eq. (6). Then the crack profile for  $x>0$  is

$$\Delta u = \frac{2\tilde{u}_\theta(\pi)\epsilon_c x_c}{(\tilde{\sigma}_e(0))^n} \frac{n}{n+2} \left[ \frac{\Delta a-x}{x_c} \right]^{(n+2)/(n+1)} \quad (21)$$

For large growth increments one obtains from eqs. (20) and (7b) for  $x>0$ :

$$\Delta u = \frac{2\tilde{u}_\theta(\pi)\epsilon_c}{(\tilde{\sigma}_e(0))^n} \frac{1}{\pi} \sin \frac{\pi n}{n+1} \int_x^{\Delta a} \left[ \frac{a'-x}{a'} \right]^{1/(n+1)} da' \quad (22)$$

The crack profiles in Fig. 2 were obtained from these equations by interpolation. As eqs. (21) and (22) show, the growing crack develops a sharp tip characterized by  $\Delta u \propto (\Delta a-x)^{(n+2)/(n+1)}$ . The overall profile resembles that of a sharp notch. A crack opening angle,  $2\beta$ , may be defined as

$$\tan\beta = \frac{\Delta u(x=0)}{2\Delta a} \quad (23)$$

For  $x=0$ , the integral in eq. (22) is equal to  $\Delta a$ , so that the crack opening angle can be calculated readily for large  $\Delta a$ . For  $n=7$ , for example, one obtains  $\tan\beta=13\epsilon_c$ . The profile in Fig. 2 was calculated with  $\epsilon_c=3\%$ , which leads to a good agreement with the observed crack profile, which is also shown in Fig. 2.

#### Consequences of Crack Blunting for the Validity of the HRR Field

In analogy to the analysis of blunting in rate-independent materials (Rice and Johnson, 1970; McMeeking and Parks, 1979), it can be concluded that the HRR field in power-law viscous material is disturbed by blunting over a distance of 3 to 5 times the crack-tip opening displacement, if crack-tip geometry changes are taken into account. This limits the allowable crack-tip opening displacement to a fraction of the crack length,  $a$ , or the ligament width,  $W-a$ , if the HRR field is to retain a finite range of approximate validity:

$$\delta_t \leq \frac{a}{2M} \quad (24)$$

Finite element calculations by McMeeking and Parks (1979) showed that the factor  $M$  has values of typically 25 for bend geometries including the CT specimen and 200 for the center-cracked plate in tension. The crack-tip opening displacement at crack growth initiation is calculated by inserting  $t=t_i$  from eq. (5) into eq. (19). For  $n=7$ , this gives

$$\delta_t = 452 \epsilon_c^{1+1/n} x_c \quad (25)$$

With  $\epsilon_c=1\%$  and  $x_c=10\mu\text{m}$ , one obtains  $\delta_t=23\mu\text{m}$ , which is sufficiently small to satisfy eq. (24) for most test specimen configurations. For a more ductile material with  $\epsilon_c=3\%$  and  $x_c=50\mu\text{m}$ , the crack-tip opening displacement is  $411\mu\text{m}$ . In this case, a CT specimen with a crack length and ligament width of 20mm would just be sufficient to satisfy eq. (24), whereas a center-cracked tension specimen should have a crack length and ligament width of at least 164mm. In specimens that are smaller than that it cannot be expected that the crack tip is surrounded by an HRR field and that crack growth rates can be transferred from one specimen to another on the basis of  $C^*$ .

#### Consequences for the Validity of the HRR Field for Growing Cracks

After crack growth initiation, the crack tip sharpens, as was shown in Fig. 2. After some growth, the crack profile approaches the notch-like geometry described by eq. (22) and by Fig. 2. It is shown next that the asymptotic stress field at a sharp notch with an included angle  $2\beta$  remains very similar to the HRR field

of a sharp crack as long as the notch angle does not become too large. Hence it can be expected that  $C^*$  remains a valid parameter despite the geometry change from the idealized mathematical crack to a notch-like profile, and that the crack growth rates are predicted accurately by the models which assume the existence of an HRR field.

To show the similarity of the crack-tip fields and the fields at a sharp notch tip, we first consider the stress and strain-rate singularities at notches,

$$\sigma \propto r^{-s}, \quad \dot{\epsilon} \propto r^{-ns}, \quad \sigma \dot{\epsilon} \propto r^{-(n+1)s}$$

where  $s$  depends on  $n$  and on the notch angle. For  $\beta=0$ , one obtains the HRR field with  $s=1/(n+1)$ . Kuang and Xu (1987) have derived numerical solutions for arbitrary notch angles. They found that for small  $\beta$  the results can be accurately described by

$$s = 2s_{e1}/(n+1) \quad (26)$$

where the linear elastic value,  $s_{e1}$ , is obtained from the eigenvalue equation

$$\sin(2(1-s)(\pi-\beta)) - (1-s)\sin 2\beta = 0 \quad (27)$$

(see, e.g., Riedel, 1987). Equation (26) is exact for  $\beta=0$  and  $n=1$ . For  $n=13$  it is accurate to 0.3% up to an angle of  $2\beta=60^\circ$ . A series-expansion solution of eq. (27) shows that  $s_{e1}$  deviates from its sharp-crack limit,  $s_{e1} = 0.5$ , only in the third order of  $\beta$ . The resulting expression,

$$s = \frac{1-\beta^3/(2\pi)}{n+1} \quad (28)$$

is accurate for all  $n$  and for moderately large  $\beta$ . It shows that the stress singularity at a notch differs from that at a crack by less than 0.3% if  $2\beta=30^\circ$  and by 2.3% if  $2\beta=60^\circ$ . The crack opening angles observed during creep crack growth are at most  $2\beta=45^\circ$  in very ductile steels.

The distribution of the stress components can be calculated in closed form in the linear case (e.g. Riedel, 1987). For small notch angles, the ratio between stress components deviates from the crack-tip fields in the second order in  $\beta$ . Directly ahead of the notch, for example, an expansion up to second order gives

$$\sigma_r/\sigma_\theta = 1-\beta^2/2. \quad (29)$$

For  $2\beta=45^\circ$ , this ratio deviates from the sharp-crack limit by 7.7%.

At a notch with a finite opening angle, the notch-analogue to the  $C^*$  contour integral, which we denote by  $N^*$ , is path dependent. For an idealized geometry of a growing crack



consisting of parallel-sided crack faces for  $x < 0$  and of a sharp V-notch for  $0 < x < \Delta a$ , as was shown in Fig. 2d, the  $N^*$  integral taken along circular paths around the notch tip can be estimated to vary as

$$N^* = C^* (r/\Delta a)^{\beta^3} / (2\pi) \quad \text{for } 0 < r < \Delta a \quad (30)$$

This approximation formula was constructed by requiring the appropriate asymptotic behavior at the notch tip defined by eq. (28) and by equating  $N^*$  to the far-field value  $C^*$  at  $r = \Delta a$ . Since the exponent in eq. (30) is small,  $N^*$  deviates very little from  $C^*$  even at distances very close to the crack tip. For  $2\beta = 45^\circ$  and  $r/\Delta a = 1/1000$ ,  $N^*$  is only 6% smaller than  $C^*$ .

In conclusion, all features of the fields near sharp notches with notch angles  $2\beta \leq 45^\circ$  are sufficiently similar to those of crack-tip fields, so that it appears reasonable to use  $C^*$  for describing creep crack growth even in the presence of considerable changes of the crack-tip geometry.

### THREE-DIMENSIONAL ASPECTS

In the past few years, three-dimensional analyses of the deformation fields in cracked bodies have become available. Owing to the viscous-elastic analogy many of the results developed for elastic-plastic materials can be applied to creeping materials as well.

Several workers have analyzed test specimen configurations such as the CT specimen with and without side grooves, with straight and with curved crack fronts, and with and without modelling crack growth (e.g. deLorenzi and Shih, 1983; Kikuchi and Miyamoto, 1984; Kienzler and Hollstein, 1987). Others have analyzed semi-elliptical surface cracks in plates and pipes (Kumar et al. 1984; Smith, Webster and Hyde, 1988; Hollstein and Kienzler, 1988; see also Schmitt, Kienzler and Hollstein; Sommer, this conference).

A convenient reference solution for surface cracks is the approximate, but accurate, solution of He and Hutchinson (1981) for the penny-shaped crack in an infinite body of power-law material:

$$C^* = \frac{6}{\pi} (1+3/n)^{-1/2} a A \sigma_e^{n-1} \sigma_I^2 \quad (31)$$

where  $\sigma_I$  is the tensile stress normal to the crack plane and  $\sigma_e$  is the von Mises equivalent stress. (In the derivation of eq. (31) an equi-biaxial transverse stress is admitted besides the tensile stress). Introducing the displacement between the crack faces in the center of the crack,  $\delta$ , gives

$$C^* = \frac{\pi}{4} \delta \sigma_I \quad (32)$$

For a semi-circular surface crack, Heitmann et al (1984) suggested to multiply eq. (31) by a factor 1.25, which accounts for the difference between an embedded crack and a surface crack in plane strain in linear elasticity. Indeed this approximates the finite element results of Smith et al. (1988) for  $n = 11.68$  to within 2 to 4%.

In evaluating three-dimensional finite element solutions, the following theoretical points of view should be kept in mind, which were discussed by Riedel (1987). Figure 3 schematically shows the distribution of the stress field on the ligament ahead of a crack in a power-law material. If crack-tip blunting is neglected beforehand, the asymptotic field near the crack front is the plane-strain HRR field. Plane strain must be approached asymptotically since the  $x_1$ - and  $x_2$ -components of strain diverge for  $r \rightarrow 0$ , while the  $x_3$ -component remains bounded and can therefore be neglected asymptotically.

In the center of the specimen the range of validity of the plane-strain HRR field may either be bounded by the transition to the plane-stress HRR field if the specimen is relatively thin, or by the transition to the plane-strain far fields if the specimen is very thick. The case of a relatively thin specimen is shown in Fig. 3. Here the transition occurs at a distance which scales with the specimen thickness, whereas for thick specimens the plane-strain HRR field is valid in a zone that scales with the crack length or ligament width.

The point where the crack front intersects the surface is called a vertex. At the vertex the range of validity of the plane-strain HRR field shrinks to zero. A new type of singularity develops at the vertex,  $\sigma \propto \rho^{-s}$ , where  $\rho$  is the distance from

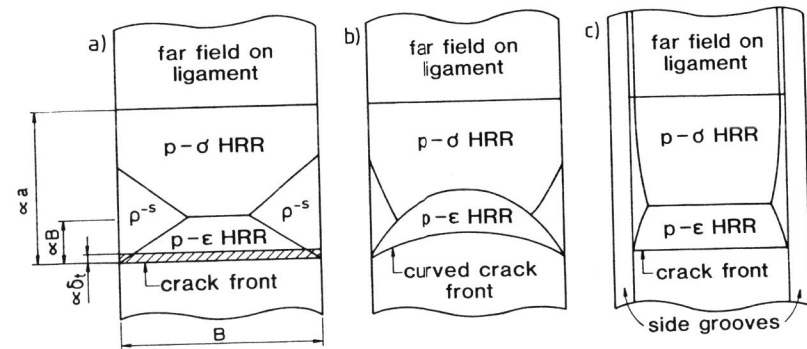


Fig. 3. Schematic of the three-dimensional stress distribution ahead of the crack for straight and curved crack fronts and for side-grooved specimens.  $p-\epsilon$  = plane strain,  $p-\sigma$  = plane stress.

the vertex, and the exponent  $s$  depends on  $n$ , and on the angle at which the crack front hits the surface. For linear elastic material and for a perpendicular crack front on the surface, Benthem (1977, 1980) has developed numerical solutions. For incompressible material (Poisson's ratio  $\nu=0.5$ ) is  $s=0.332$ , and for  $\nu=0.3$  is  $s=0.452$ .

Bazant and Estenssoro (1979) explore the effect of the angle between the crack front and the surface in elastic materials. They find that a square-root singularity,  $s=1/2$ , which prevails in the bulk, is established also at the vertex if the crack front deviates by  $11^\circ$  from being normal on the surface if  $\nu=0.3$ , and by about  $20^\circ$  if  $\nu=0.5$ . Accordingly a growing crack front tends to establish a shape making such an angle with the free surface, since a uniform stress singularity along the crack front is a necessary (but not sufficient) prerequisite for a uniform stress intensity factor (or  $J$  integral) and for a uniform growth rate. This effect is called crack tunnelling (Fig. 3b). In nonlinear material, the vertex singularities have not been evaluated, but experimental and numerical investigations indicate that crack tunnelling must be more pronounced in nonlinear material in order to establish a uniform distribution of  $J$  or  $C^*$  and a uniform growth rate along the crack front.

Sharp side grooves are expected to raise the value of the exponent  $s$  of the vertex singularity. From finite element calculations of deLorenzi and Shih (1983) it appears that a side-groove angle of  $45^\circ$  gives an approximately uniform stress singularity for both elastic and power-law hardening material. Hence the  $J$  integral is relatively constant along the crack front for an appropriate choice of the side groove depth, and the range of validity of the plane-strain field is extended near the vertex, as is shown schematically in Fig. 3c. Correspondingly, growing cracks tend to develop a straight front in side-grooved specimens.

So far, the fields were discussed neglecting crack-tip geometry changes. As described earlier, blunting disturbs the fields over a distance that scales with the crack-tip opening displacement,  $\delta_t$ . The disturbed zone is shown schematically as the hatched area in Fig. 3. If the hatched area is larger than the regime of the plane-strain field, the local fracture processes occur under plane-stress conditions. Otherwise, the fracture processes occur in a zone deformed in plane strain. Contrary to a frequent misconception, plane-strain conditions near the crack tip do not imply that the far fields and the load-displacement response of the specimen must also be close to plane strain.

#### CONTINUUM DAMAGE MECHANICS

In the models for creep crack growth described earlier cavitation ahead of the crack was assumed to occur in the undisturbed HRR field which prevails in a power-law viscous material. In a damage-mechanics model, on the other hand, the effect of damage on the stress distribution is taken into account.

#### The Kachanov-Rabotnov Equations

The classical damage-mechanics equations are those of Kachanov and Rabotnov. A damage parameter,  $\omega$ , is introduced which varies from 0 for the undamaged material to 1 at fracture. This is described by the evolution law

$$\dot{\omega} = \frac{D\sigma^\chi}{(1+\phi)(1-\omega)^\phi} \quad (33)$$

Here,  $D$ ,  $\chi$ , and  $\phi$  are material parameters. The enhancement of the creep strain rate by damage is described by the equation

$$\dot{\epsilon}_{cr} = \frac{A\sigma^n}{(1-\omega)^n} \quad (34)$$

This pair of equations is an empirical means to describe the stress/strain-rate response especially in the tertiary stage of creep. The damage parameter is an internal variable with no physical meaning, although it is somehow, but not in a strict sense, related to the cavitated area fraction of grain boundaries.

A possible generalization of eqs. (33) and (34) to multiaxial states of stress has been worked out by Hayhurst and Leckie (1984). This problem will not be addressed here. Although the details of the field distributions depend on the multiaxial form of the constitutive equations, some essential features can be derived already from the uniaxial form.

Other damage-mechanics models and their applications to creep crack growth will be described in a later section.

#### Two General Remarks

It is interesting to note that crack growth is automatically contained in solutions of eqs. (33) and (34). Wherever  $\omega$  reaches 1, the stiffness of the material is zero, i.e. the material has failed locally, i.e. the crack has propagated. No separate crack growth criterion, such as a critical-strain criterion is needed, and the theory contains no structural length,  $x_c$ .

A second remark refers to the range of validity of  $C^*$ -controlled creep crack growth in the framework of continuum damage mechanics. One may expect that a small-scale damage limit can be defined, in which the stress field is determined by viscous creep in almost the whole specimen except in a small zone near the crack tip, which is called the process zone and in which the stress field is strongly affected by the presence of damage. Such a situation is expected to dominate at short times. Later the process zone spreads over the whole ligament of the specimen. Only in the small-scale damage limit is the process zone encompassed by a nearly undisturbed HRR field. Hence crack

growth rates in specimens of different sizes and shapes can be compared on the basis of  $C^*$  only in this limiting case.

In the large-scale damage range, crack growth rates cannot be transferred from test specimens to differently shaped components using  $C^*$ . A full finite element analysis based on the damage-mechanics equations is then necessary for each component. Such calculations were performed by Hayhurst, Brown and Morrison (1984). However, this procedure is not only expensive and time consuming, but it may also lead to serious error. If the local failure of material at the crack tip is accelerated by corrosive processes, the crack will actually grow faster than predicted by the damage-mechanics equations which do not contain local corrosion. On the other hand, if the crack growth rates measured in the appropriate atmosphere are transferred to the component using the appropriate load parameter, the corrosive effect is properly accounted for. In such a case, a fracture-mechanics treatment on the basis of  $C^*$  will be superior to a full damage-mechanics analysis. It remains to explore the range of validity of the small-scale damage approximation which is a prerequisite for the transferability of crack growth rates by  $C^*$ .

#### The Growth of a Process Zone and of the Crack in an Extensively Creeping Specimen

The small-scale damage problem in an extensively creeping specimen can be formulated as a boundary layer problem. The crack is considered as being of semi-infinite length and the stress must approach the HRR field of the non-damaging material at large distances from the crack tip (large compared to the process zone size, which will be calculated, but small compared to the crack length and ligament width). The initial condition at the time of load application,  $t=0$ , is the field in a viscous, non-damaging material. For these initial and remote boundary conditions, Riedel (1985b, 1987) has shown that the governing equations, eqs. (33) and (34) together with the equilibrium and compatibility equations, have similarity solutions for the stress, strain-rate, and damage fields. All features of the fields, including the process zone and the current crack tip expand around the original crack tip according to

$$\Delta a \propto r_{pr} \propto (C^*/A)(Dt)^{(n+1)/\chi}, \quad (35)$$

where  $r_{pr}$  is the process zone size. The precise definition of the process zone is somewhat arbitrary. For example, one may define the process zone boundary where the equivalent strain rate is doubled by damage compared to non-damaging viscous material. The factors of proportionality in eq. (35) cannot be derived from the dimensional considerations, which give the general form of eq. (35). Upper- and lower-bound estimates, as well as a calculation by the finite element method were given by Riedel (1985b).

If eq. (35) is differentiated with respect to time and rearranged one recognized that the crack growth rate is the same as in eq. (7) apart from a numerical factor. For the comparison

one should set  $\chi = n$ , which implies strain-controlled local failure. Hence in this case the damage-mechanics model leads to practically the same result as the model in which the effect of damage on the stress field was neglected.

The stress distribution in the process zone was calculated by Riedel (1985b) using the finite element method. As one would expect, the stress is completely relaxed at the current crack tip. Within the process zone, which is of the same order of magnitude as  $\Delta a$ , the stress increases and approaches the HRR field quickly outside the process zone.

#### The Range of Validity of the Small-Scale Damage Approximation

The disturbance of the HRR field by the process zone is quite analogous to the disturbance by crack-tip blunting. The disturbance now extends over a length which is about equal to the amount of crack growth,  $\Delta a$ . Hence  $\Delta a$  should be limited to about 10% of the initial crack length or ligament width. Otherwise the HRR field has no finite range of validity and  $C^*$  cannot be used as a correlating parameter. For long cracks in typical test specimen configurations, 10% crack extension correspond to 60 to 80% of the lifetime, so that  $C^*$  is a valid parameter for a large fraction of the lifetime. For short cracks, however, one expects that the range of validity of  $C^*$  ends at a small fraction of the lifetime due to wide-spread damage.

It should be kept in mind, however, that this limitation to  $C^*$  is derived from a specific theoretical model. If the model contained a nucleation stress which must be attained before damage accumulation can start, the process zone would not continue to grow in proportion to  $\Delta a$  for larger  $\Delta a$ . In such a model, the range of validity of  $C^*$  would be less restricted.

As an engineering solution to the problem of small cracks, Webster *et al.* (1986) propose to calculate the lifetime by interpolation between the result of a reference-stress concept, which is appropriate for short cracks, and the result of a calculation based on  $C^*$ , which is appropriate for longer cracks. A full damage-mechanics finite element calculation could also resolve the problem, apart from the fact that crack growth by local corrosion cannot be described, as was already mentioned.

#### Growth of the Crack Within a Small Creep Zone

In a material model that includes elastic strain rates according to

$$\dot{\epsilon} = \frac{\dot{\sigma}}{E} + \frac{A\sigma^n}{(1-\omega)^n}, \quad (36)$$

the process zone and the crack may either grow inside the creep zone or may overtake the growing creep zone. The first case is considered here, while the latter is discussed in the next section.

If the crack tip and the process zone grow well within a creep zone which is itself small compared to the specimen dimensions, a boundary layer problem can be formulated with the remote boundary condition being the HRR field, eq. (10), with the short-time limit of eq. (11) for  $C(t)$  inserted. This problem again has similarity solutions. The crack and the process zone expand around the original crack tip as described by eq. (35) but with  $C^*$  replaced by  $C(t) \propto K_I^2/Et$ . Hence, also in this case the crack growth rate is the same as in the model based on a critical-strain criterion, which neglects the disturbance of the stress field by damage. Again there will be a smooth transition to crack growth in an extensively creeping specimen as described by eq. (7) with  $C^*$  replaced by  $C(t)$  from eq. (11), unless the crack overtakes the creep zone before the extensive creep limit is reached.

#### Crack and Process Zone Growing Outside the Creep Zone

##### ( $K_I$ -Controlled Growth Under Small-Scale Creep Conditions)

If the crack grows faster than the creep zone, the process zone is directly embedded in the elastic singular field. This means that there is no creep zone, and creep strains are important only where they are significantly enhanced by damage.

For this case, Riedel (1988) has developed similarity solutions in which the crack expands according to

$$\Delta a \propto K_I^2 \left[ \frac{(EA)^{\phi+1} t^{\phi+1-n}}{D^n} \right]^{2/(n-1)(\phi+1)-n\chi} \quad (37)$$

Since this solution was derived assuming that the crack had overtaken the creep zone, it can only be valid if  $\Delta a > r_{cr}$ . This and other requirements for the validity of the solutions have been evaluated by Riedel (1988). No complete picture could be obtained, since in certain regimes of time and material parameters the solutions were contradictory.

It is not yet clear whether or not a solution of the damage-mechanics equations exists for a constant crack growth rate under small-scale creep conditions. No arguments could be found that no such steady-state solution should exist, but no such solution has actually been constructed. However, from simple dimensional reasons it is clear that, if a steady-state solution exists, the crack growth rate must be proportional to  $K_I^2$ . Older theories based on a critical-strain criterion had given  $\dot{a} \propto K_I$  (e.g. Hui and Riedel, 1981). Experimental results (e.g. Riedel and Wagner, 1984) tend to support the stronger dependence predicted by the older theory.

Further, it turned out that the irregularities in crack growth rate that had been found in models based on a critical-strain criterion (Hui and Riedel, 1981; Riedel and Wagner, 1981; Wu, Bassani and Vitek, 1986) could not be found in the damage-mechanics model. The reason for this is that the singular field

at a growing crack in elastic/power-law viscous material (Hui and Riedel, 1981) plays a role and causes irregular growth in the older models based on critical strain, whereas it has no range of validity in the damage-mechanics model.

In conclusion, the theory of creep crack growth under small-scale creep conditions is less well understood theoretically than creep crack growth under extensive creep conditions or during the transients to extensive creep.

#### Other Damage Mechanics Models

Several authors have tried to develop model-based damage-mechanics equations and to apply them to problems involving macroscopic cracks. Most of them start from a model proposed by Hutchinson (1983). He argues that under a wide range of conditions cavity growth is constrained (Dyson, 1976, 1979; Rice, 1981), which means that the cavitating grain boundary facets behave like microcracks in the sense that they transmit no tractions. Consequently, Hutchinson models a cavitating creeping solid as a power-law viscous material containing a distribution of penny-shaped microcracks. He carries out the analysis for a small number density of microcracks and obtains (for uniaxial tension):

$$\dot{\epsilon} = A(1+\omega)\sigma^n \quad (38)$$

Now the damage parameter has the well-defined meaning

$$\omega = \frac{n+1}{2(1+3/n)^{1/2}} d^3 N_{mc} \quad (39)$$

with the diameter  $d$  of the microcracks and their number density  $N_{mc}$ . No attempts were made by Hutchinson to provide an evolution law for  $\omega$ . This part of the problem must probably be solved empirically, for example by adjusting the parameters of the evolution law, eq. (33), to experimental data.

Hutchinson's (1983) constitutive model has been extended to larger concentrations of microcracks by Riedel (1987). If a self-consistent argument is worked out in a very simple, one-dimensional manner, one obtains

$$\dot{\epsilon} = \frac{A\sigma^n}{1-\omega} \quad (40)$$

This differs from the Kachanov-Rabatnov formulation, eq. (34), by the missing exponent  $n$  in the denominator.

Instead of the conventional self-consistent method, one can employ the differential self-consistent method (see, e.g., Duva, 1984). If applied in the same approximate manner as above, the differential scheme gives

$$\dot{\epsilon} = e^{\omega} A\sigma^n \quad (41)$$

An exact, but numerical evaluation of the differential self-consistent scheme by Rodin and Parks (1986) suggests that eq. (41) overestimates interaction effects between the microcracks. Their numerical results can be approximated more closely (to within 2% up to  $\omega = 1$  for  $n = 3$ ) if one assumes that crack interactions occur only through the deviatoric part of Hutchinson's result, whereas the dilatations due to the cracks are simply additive. This leads to

$$\dot{\epsilon} = \left[1 + \frac{2\omega}{n+1}\right] e^{(n-1)\omega/(n+1)} A\sigma^n \quad (42)$$

in uniaxial tension.

These approximate self-consistent estimates are useful in providing the constitutive equations in analytical form. Their accuracy should be checked by comparison with periodic or cell models which are treated by finite elements. A first comparison of eq. (40) with numerical results of Tvergaard (1984a,b) for  $n = 5$  and  $\omega = 0.38$  gave a good agreement to within 1%. In this case, the strain rate predicted by eqs. (41) and (42) is 10% low, and the dilute estimate, eq. (38), is 15% low.

Bassani and Hawk (1987) have summarized the three-dimensional forms of some of these constitutive laws and have added another one. They have also described methods to solve the damage mechanics equations for crack growth problems by the finite element method, and have provided first numerical solutions.

Tvergaard (1986) has also developed finite element solutions of damage-mechanics equations for crack geometries. He uses a constitutive model similar to that of Hutchinson (1983) which is valid for a dilute concentration of microcracks. He combines the constitutive model with an imposed crack growth criterion, which is not needed in Kachanov-type models.

A common feature of most, if not all, of these damage-mechanics models is that they allow for similarity solutions in the small-scale damage limit, just as does the Kachanov model. Finite element results should be checked whether they are compatible with the required similitude of the fields. On the other hand, they should be evaluated for the range of validity of the similarity solutions which defines the range of validity of the respective load parameters such as  $C^*$ .

#### LOAD PARAMETER MAPS

Load parameter maps are diagrams with reference stress (or net section stress) on the horizontal axis and time on the vertical axis (Riedel, 1985a, 1987). A schematic is shown in Fig. 4. On this map the regimes are shown in which different load parameters -  $K_I$ ,  $J$ ,  $C_h$ ,  $C^*$  - determine the crack growth behavior. The lines separating these regimes represent the characteristic times  $t_1$  and  $t_2$  given in earlier sections. Crack-tip blunting gives another line denoted by  $t_b$  bounding the ranges of validity of  $C^*$  and of  $J$ . Finally, the regime of  $C^*$  is bounded by the

growth of a process zone at a certain fraction of the lifetime (the hatched band in Fig. 4).

Such a load parameter map was constructed for CT specimens of a ferritic steel at 540°C by Riedel and Detampel (1987). The location of the boundaries on the map depends on material, temperature and specimen shape, but not on the specimen size. The effect of specimen shape is small if the reference stress is used on the horizontal axis.

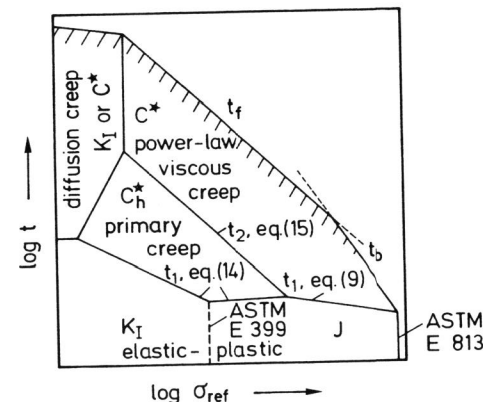


Fig. 4. Load parameter map (schematic). Copyright ASTM. Reprinted with permission.

#### SUMMARY

If a material behaves as a nonlinear viscous solid,  $C^*$  is the appropriate load parameter to describe creep crack growth. This has been confirmed experimentally for many creep-ductile materials.

Measured crack growth rates can be explained by models in which the micromechanism of failure is assumed to be strain controlled (e.g. constrained grain boundary cavitation). The crack growth rate is predicted to vary as  $\dot{a} \propto C^*n/(n+1)$  and to depend on the amount of crack growth,  $\Delta a$ ; for large  $\Delta a$  is  $\dot{a} \propto \Delta a^{1/(n+1)}$ .

Crack-tip blunting and the geometry changes during crack growth have been described, and conclusions have been drawn regarding the range of validity of  $C^*$  in the presence of blunting.

The three-dimensional field distribution ahead of a crack has been discussed. Near the crack front the field approaches a plane-strain field unless the disturbance by blunting has a

greater range than the plane-strain field.

At short times the range of validity of  $C^*$  is bounded by elastic-plastic deformations. Here  $K_I$  or  $J$  predominate.

The crack-growth behavior during the transient from the elastic-plastic response to steady-state creep can be described by the crack-tip parameter  $C(t)$ , which is approximated by the easily measurable parameter  $C_t$ . The same is true for primary creep.

Tertiary creep is included in the form of a damage-mechanics description. This leads to calculated crack growth rates which practically agree with those obtained earlier from a critical-strain criterion. Further the damage-mechanics model specifies the limitation to  $C^*$  due to wide-spread damage.

The ranges of validity of different load parameters can be shown on a load parameter map.

The modelling of creep crack growth under small-scale creep conditions has not been entirely successful. Slightly different models lead to very different predictions of the crack growth behavior.

The effects of corrosion on creep crack growth have not yet been modelled.

For practical purposes it would be desirable to enhance experimental and theoretical work on creep crack growth in welds and in their heat-affected zones.

#### REFERENCES

- Bassani, J.L. (1981). In: *Creep and Fracture of Engineering Materials and Structures* (B. Wilshire and D.R.J. Owen, eds.), pp. 329-344, Pineridge Press, Swansea.
- Bassani, J.L. and D.E. Hawk (1987). In: *Proceedings of Mecamat International Seminar on High Temperature Fracture Mechanisms and Mechanics*, Dourdan, France (P. Bensussan et al., eds.), pp. 19-40, Mecamat, Moissy-Cramayet.
- Bazant, Z.P. and L.F. Estenssoro (1979). *Int. J. Solids Structures* **15**, 405-426.
- Benthem, J.P. (1977). *Int. J. Solids Structures* **13**, 479-492.
- Benthem, J.P. (1980). *Int. J. Solids Structures* **16**, 119-130.
- deLorenzi, H.G. and C.F. Shih (1983). *Int. J. Fracture* **21**, 195-220.
- Duva, J.M. (1984). *J. Eng. Mater. Technology* **106**, 317-321.
- Dyson, B.F. (1976). *Metal Sci.* **10**, 349-353.
- Dyson, B.F. (1979). *Canad. Metall. Qu.* **18**, 31-38.
- Earthman, J.C., J.C. Gibeling and W.D. Nix (1985). *Acta Metall.* **33**, 805-817.
- Ehlers, R. (1981). PhD Thesis. Fakultät für Bergbau und Hüttenwesen der Rheinisch-Westfälischen Technischen Hochschule Aachen.
- Ehlers, R. and H. Riedel (1981). In: *Advances in Fracture Research, Proceedings of ICF5* (D. Francois et al., eds.), Vol. 2, pp. 691-698, Pergamon Press, Oxford and New York.
- Evans, A.G. and W. Blumenthal (1982). *Fracture Mechanics of Ceramics* (R.C. Bradt et al., eds.), Vol. 5, Plenum, New York.
- Floreen, S. (1983). In: *Elastic-Plastic Fracture: Second Symposium, ASTM STP 803* (C.F. Shih and J.P. Gudas, eds.), Vol. I-Inelastic Analysis, pp. I-708-I-720, American Society for Testing and Materials.
- Gooch, D.J. (1982). *Metal Sci.* **16**, 79-89.
- Harrison, C.B. and G.N. Sandor (1971). *Eng. Fracture Mech.* **3**, 403-420.
- Hayhurst, D.R., P.R. Brown and C.J. Morrison (1984). *Phil. Trans. Roy. Soc. Lond. A* **311**, 131-158.
- Hayhurst, D.R. and F.A. Leckie (1984). In: *Mechanical Behaviour of Materials*, Proceedings of ICM4 (J. Carlsson and N.G. Ohlson, eds.), Vol. 2, pp. 1195-1212, Pergamon Press, Oxford.
- He, M.Y. and J.W. Hutchinson (1981). *J. Appl. Mech.* **48**, 830-840.
- Heitmann, H.H., H. Vehoff and P. Neumann (1984). In: *Advances in Fracture Research '84 - Proceedings of ICF6*, (S.R. Valluri et al., eds.), Vol. 5, pp. 3599-3606, Pergamon Press, Oxford and New York.
- Hollstein, T. and R. Kienzler (1988). *J. Strain Analysis* **23**, 87-96.
- Hui, C.Y. and H. Riedel (1981). *Int. J. Fracture* **17**, 409-425.
- Hutchinson, J.W. (1968). *J. Mech. Phys. Solids* **16**, 13-31.
- Hutchinson, J.W. (1983). *Acta Metall.* **31**, 1079-1088.
- Hutchinson, J.W. and P.C. Paris (1979). In: *Elastic-Plastic Fracture, ASTM STP 668*, pp. 37-64, American Society for Testing and Materials.
- Jaske, C.E. (1988). In: *Fracture Mechanics: Eighteenth Symposium, ASTM STP 945*, (D.T. Read and R.P. Reed, eds.), pp. 867-877, American Society for Testing and Materials, Philadelphia.
- Kienzler, R. and T. Hollstein (1987). In: *Creep and Fracture of Engineering Materials and Structures* (B. Wilshire and R.W. Evans, eds.), pp. 563-576, The Institute of Metals, London.
- Kikuchi, M. and H. Miyamoto (1984). In: *Proceedings of the Third International Conference on Numerical Methods in Fracture Mechanics* (A.R. Luxmoore and D.R.J. Owen, eds.), pp. 205-217, Pineridge Press, Swansea, U.K.
- Koterazawa, R. (1986). In: *International Conference on Creep*, Tokyo, April 1986, ISME, IMechE, ASME, ASTM, pp. 291-296.
- Koterazawa, R. and T. Mori (1977). *Trans. ASME, J. Eng. Mater. Technology* **99**, 298-305.
- Kuang, Z.-b. and X.-p. Xu (1987). *Int. J. Fracture* **35**, 39-53.
- Kubo, S., K. Ohji and K. Ogura (1979). *Eng. Fracture Mech.* **11**, 315-329.
- Kuhnle, V. and H. Riedel (1987). *Int. J. Fracture* **34**, 179-194.
- Kumar, V., M.D. German and C.F. Shih (1981). *An Engineering Approach for Elastic-Plastic Fracture Analysis*, Report NP-1931 on Project 1237-1 for Electric Power Research Institute, Palo Alto, California.
- Kumar, V., M.D. German, W.W. Wilkening, W.R. Andrews, H.G. deLorenzi and D.F. Mowbray (1984). *Advances in Elastic-Plastic Fracture Analysis*, NP-3607 on Project 1237-1 to Electric Power Research Institute, Palo Alto, California.
- Landes, J.D. and J.A. Begley (1976). In: *Mechanics of Crack Growth, ASTM STP 590*, pp. 128-148, American Society for Testing and Materials.
- Leung, C.-P., D.L. McDowell and A. Saxena (1988a). In: *Third International Symposium on Nonlinear Fracture Mechanics*,

- Knoxville, October 1986, to appear as an *ASTM STP*.
- Leung, C.-P., D.L. McDowell and A. Saxena (1988b). *Int. J. Fracture* **36**, 275-289.
- Li, F.Z., A. Needleman and C.F. Shih (1988). *Int. J. Fracture* **36**, 163-186.
- Maas, E. and A. Pineau (1984). In: *Mechanical Behaviour of Materials*, Proceedings of ICM4 (J. Carlsson and N.G. Ohlson, eds.), Vol. 2, pp. 763-769, Pergamon Press, Oxford.
- Maas, E. and A. Pineau (1985). *Eng. Fracture Mech.* **22**, 307-325.
- McMeeking, R.M. and D. Parks (1979). In: *Elastic-Plastic Fracture*, *ASTM STP 668* (J.D. Landes, J.A. Begley and G.A. Clarke, eds.), pp. 175-194, American Society for Testing and Materials.
- Nikbin, K.M., G.A. Webster and C.E. Turner (1976). In: *Cracks and Fracture*, *ASTM STP 601*, pp. 47-62, American Society for Testing and Materials.
- Ohji, K., K. Ogura and S. Kubo (1974). Preprint of *Japan. Soc. Mech. Engrs.*, No. 640-11, p.207 (in Japanese).
- Ohji, K., K. Ogura, and S. Kubo (1980). *J. Soc. Mater. Sci. Japan* **29**, No. 320, 465-471.
- Ohji, K., K. Ogura, S. Kubo and Y. Katada (1978). In: *Proceedings the 21st Japan Congress on Materials Research*, pp. 99-104, The Society of Materials Science Japan, Kyoto.
- Ohji, K., K. Ogura, S. Kubo and Y. Katada (1980). In: *Engineering Aspects of Creep*, Vol. 2, pp. 9-16, The Institution of Mechanical Engineers, London.
- Radhakrishnan, V.M. and A.J. McEvily (1980). *Z. Metallkde.* **71**, 133-137.
- Rice, J.R. (1968). *ASME J. Appl. Mech.* **35**, 379-386.
- Rice, J.R. (1981). *Acta Metall.* **29**, 675-681.
- Rice, J.R. and M.A. Johnson (1970). In: *Inelastic Behavior of Solids* (M.F. Kanninen et al., eds.), pp. 641-671, McGraw-Hill, New York.
- Rice, J.R. and G.F. Rosengren (1968). *J. Mech. Phys. Solids* **16**, 1-12.
- Riedel, H. (1981a). In: *Creep in Structures* (A.R.S. Ponter and D.R. Hayhurst, eds.), pp. 504-519, Springer-Verlag, Berlin, Heidelberg, New York.
- Riedel, H. (1981b). *J. Mech. Phys. Solids* **29**, 35-49.
- Riedel, H. (1985a). In: *Flow and Fracture at Elevated Temperatures* (R. Raj, ed.), pp. 149-177, American Society for Metals, Metals Park, Ohio.
- Riedel, H. (1985b). In: *Fundamentals of Deformation and Fracture* (B.A. Bilby, K.J. Miller and J.R. Willis, eds.), pp. 293-309, Cambridge University Press, Cambridge.
- Riedel, H. (1987). *Fracture at High Temperatures*, Springer-Verlag, Berlin Heidelberg New York.
- Riedel, H. (1988). Paper presented at IUTAM Symposium on Recent Advances in Nonlinear Fracture Mechanics. Proceedings to be published in *Int. J. Fracture*.
- Riedel, H. and V. Detampel (1987). *Int. J. Fracture* **33**, 239-262.
- Riedel, H. and J.R. Rice (1980). In: *Fracture Mechanics: Twelfth Conference*, *ASTM STP 700* (P.C. Paris, ed.), pp. 112-130, American Society for Testing and Materials.
- Riedel, H. and W. Wagner (1981). In: *Advances in Fracture Research - Proceedings of ICF5* (D. Francois et al., eds.), Vol. 2, pp. 683-688, Pergamon Press, Oxford and New York.
- Riedel, H. and W. Wagner (1984). In: *Advances in Fracture Research - Proceedings of ICF6* (S.R. Valluri et al., eds.), Vol. 3, pp. 2199-2206, Pergamon Press, Oxford and New York.
- Rodin, G.J. and D.M. Parks (1986). *Mech. Mater.* **5**, 221-228.
- Sadananda, K. and P. Shahinian (1980a). *Mater. Sci. Eng.* **43**, 159-168.
- Sadananda, K. and P. Shahinian (1980b). *Metall. Trans.* **11A**, 267-276.
- Sadananda, K. and P. Shahinian (1983). *Metall. Trans.* **14A**, 1467-1480.
- Saxena, A. (1980). In: *Fracture Mechanics: Twelfth Conference*, *ASTM STP 700* (P.C. Paris, ed.), pp. 131-151, American Society for Testing and Materials.
- Saxena, A. (1986). In: *Fracture Mechanics: Seventeenth Symposium*, *ASTM STP 905* (J.H. Underwood et al., eds.), pp. 185-201, American Society for Testing and Materials.
- Saxena, A. and J.D. Landes (1984). In: *Advances in Fracture Research - Proceedings of ICF6* (P. Rama Rao et al., eds.), Vol. 6, pp. 3977-3988, Pergamon Press, Oxford and New York.
- Shih, C.F. (1983). *Tables of the Hutchinson-Rice-Rosengren Singular Field Quantities*, Brown University Report MRL E-147, Providence, R.I.
- Siverns, M.J. and A.T. Price (1970). *Nature* **228**, 760-761.
- Smith, S.D., J.J. Webster and T.H. Hyde (1988). *Eng. Fracture Mech.* **30**, 105-116.
- Speidel, M.O. (1981). In: *Advances in Fracture Research - Proceedings of ICF5* (D. Francois et al., eds.), Vol. 6, pp. 2685-2704, Pergamon Press, Oxford and New York.
- Taira, S., R. Ohtani and T. Kitamura (1979). *Trans. ASME, J. Eng. Mater. Technology* **101**, 154-161.
- Tvergaard, V. (1984a). *J. Mech. Phys. Solids* **32**, 373-393.
- Tvergaard, V. (1984b). *Acta Metall.* **32**, 1977-1990.
- Tvergaard, V. (1986). *Int. J. Fracture* **31**, 183-209.
- Viswanathan, R., R. Dooley and A. Saxena (1988). In: *Proceedings of the International Conference on Life Assessment and Extension*, The Hague, pp. 173-184, VGB, Essen, Germany.
- Webster, G.A., D.J. Smith and K.M. Nikbin (1986). In: *International Conference on Creep*, Tokyo, pp. 303-308, Japanese Society of Mechanical Engineers.